On the Maslov index of multi-pulse homoclinic orbits

By Frédéric Chardard[1], Frédéric Dias[1], Thomas J. Bridges[2]

1. CMLA, École Normale Supérieure de Cachan, CNRS, PRES UniverSud, 61 Av. President Wilson, F-94230 Cachan, France

2. Department of Mathematics, University of Surrey, Guildford GU2 7XH, UK

Multi-pulse homoclinic orbits of Hamiltonian systems on $\mathbb{R}^4$ can be classified by a sequence of integers. In this paper we find the surprising result that this string of integers encodes the value of the Maslov index of the homoclinic orbit. Our results include a computable formulation of the Maslov index for homoclinic orbits and a robust numerical method for the evaluation of the Maslov index.

Keywords: Hamiltonian systems, Lagrangian planes, Maslov index, exterior algebra, geometric numerical integration, bifurcation

1. Introduction

Homoclinic orbits are important in Hamiltonian dynamical systems. They can be organizing centres for chaos, and in the case where they are steady-state solutions of an evolutionary PDE they represent localized solutions such as solitary waves. Of interest in this paper are multi-pulse homoclinic orbits.

A multi-pulse homoclinic orbit is firstly a homoclinic orbit. The "multi-pulse" nature indicates multiple maxima and minima in the graph of the function. An important open question is how to distinguish between two multi-pulse homoclinic orbits. A universal classification of multi-pulse homoclinic orbits has yet to emerge. However, for a class of autonomous Hamiltonian systems on $\mathbb{R}^4$, Buffoni, Champneys & Toland (1996) have introduced a precise classification based on a sequence of integers. Multi-pulse homoclinic orbits are labelled by $\mathbf{n}(\ell_1, \ldots, \ell_{n-1})$ where $\mathbf{n}$ is the modality (the number of major local extrema) and $\ell_1, \ldots, \ell_{n-1}$ are related to the number of minor bumps between consecutive extrema. A precise definition is given in Buffoni et al. (1996). Hereafter this classification is called the BCT classification.

An important topological invariant of any orbit of a Hamltonian system is the *Maslov index*. A precise definition of Maslov index in this context is given in §2. We have found that the Maslov index of a homoclinic orbit is encoded in the BCT classification:

$$\mathsf{Maslov}^{\text{homoclinic}} = n_{even} + 2n_{odd} + 2\,, \tag{1.1}$$

where n_{even} (n_{odd}) is the number of even (odd) integers in the sequence $\ell_1, \ldots, \ell_{n-1}$. This observation is numerical. The results are obtained by explicit computation using a new numerical algorithm for computing the Maslov index.

The class of Hamiltonian systems of interest is steady solutions of the PDE

$$\phi_t = -\phi_{xxxx} - P\phi_{xx} - \phi + \phi^2\,, \tag{1.2}$$

where P is a real parameter. Steady solutions are orbits of the ODE

$$\phi_{xxxx} + P\phi_{xx} + \phi - \phi^2 = 0\,. \tag{1.3}$$

This ODE has been extensively studied because of its importance in pattern formation. It is called the canonical equation in the book by Peletier & Troy (2001), and it is the ODE that forms the basis of the theory of Buffoni et al. (1996). The ODE (1.3) can be characterized as a Hamiltonian system and the formulation used here is recorded in Appendix A.

The PDE (1.2) arises in many applications: beam buckling, pattern formation – where it is called the one-dimensional Swift-Hohenberg equation (Burke & Knobloch 2007), thin film flows, and a variant (an additional space derivative is added to the right-hand side) arises in the theory of capillary-gravity water waves, called the fifth-order KdV equation. A review of equations of this type is given by Champneys (1999).

The linearization of (1.2) about a multi-pulse solution $\widehat{\phi}(x)$ satisfying (1.3) and taking exponential in time solutions $\phi(x,t) \mapsto \mathrm{e}^{-\lambda t}\phi(x)$ leads to the linear ODE

$$\phi_{xxxx} + P\phi_{xx} + \phi - 2\widehat{\phi}(x)\phi = \lambda\phi\,. \tag{1.4}$$

This ODE can be reformulated as a standard linear Hamiltonian system on $\mathbb{R}^4$,

$$\mathbf{J}\mathbf{u}_x = \mathbf{B}(x,\lambda)\mathbf{u}\,, \quad \mathbf{u} \in \mathbb{R}^4\,, \tag{1.5}$$

where $\mathbf{B}(x,\lambda)$ is a symmetric matrix depending smoothly on x and λ with the property that

$$\lim_{x\to\pm\infty} \mathbf{B}(x,\lambda) = \mathbf{B}_\infty(\lambda)\,, \tag{1.6}$$

and

$$\mathbf{J} = \begin{bmatrix} \mathbf{0} & -\mathbf{I} \\ \mathbf{I} & \mathbf{0} \end{bmatrix}\,. \tag{1.7}$$

The matrix $\mathbf{B}(x,\lambda)$ is defined in Appendix A in equation (A 2).

The parameter λ serves two purposes. It is a stability exponent for the PDE, but it is also a device for assuring genericity (see §2a for discussion). We will be primarily interesting in the limit $\lambda \to 0$.

The Maslov index is most familiar in the literature in the context of closed orbits, e.g. the case of (1.5) with periodic coefficients, because of its importance in semi-classical quantization (cf. Arnold (1967), Littlejohn (1986), Littlejohn & Robbins (1987), Robbins (1991), Pletyukhov & Brack (2003) and references therein). The Maslov index of homoclinic orbits was first introduced by Jones (1988) and Bose & Jones (1995) for 1−pulse homoclinic orbits. We turn this definition into a computable formula by introducing an explicit intersection form, following Robbins (1991,1992) and Robbin & Salamon (1993). Chen & Hu (2007) have recently introduced a formulation of the Maslov index for homoclinic orbits. They give two constructions. The first is based on an intersection index and therefore is a generalization of the Bose-Jones definition. Their second definition is based on a relative Morse index of (1.5) considered as an operator on the real line. It is the intersection index formulation that is most useful for numerics.

The Maslov index for a homoclinic orbit can also be defined by approximating the homoclinic orbit by a periodic orbit and then taking the limit as the period of the orbit goes to infinity. The existence of this Maslov index was recently proved in Chardard (2007). Both definitions are used in the numerical computation in order to double check the results.

The paper has three parts: derivation of a computable formula for the Maslov index, a numerical algorithm on exterior algebra spaces for computing the Maslov index, and results for multi-pulse orbits of (1.3).

2. The Maslov index of a homoclinic orbit

A subspace $\mathrm{span}\{\xi_1, \xi_2\}$ of $\mathbb{R}^4$ is a Lagrangian subspace if ξ_1 and ξ_2 are linearly independent and $\langle \mathbf{J}\xi_1, \xi_2\rangle = 0$. Here and throughout $\langle \cdot, \cdot \rangle$ is the standard inner product on $\mathbb{R}^4$. The stable and unstable subspaces of (1.5) are Lagrangian subspaces.

The matrix $\mathbf{A}_\infty(\lambda) := \mathbf{J}^{-1}\mathbf{B}_\infty(\lambda)$ and $\mathbf{B}_\infty(\lambda)$ is defined in (A 3) in Appendix A. The characteristic polynomial of $\mathbf{A}_\infty(\lambda)$ is

$$\det[\mathbf{A}_\infty(\lambda) - \mu\mathbf{I}] = \mu^4 + P\mu^2 + 1 - \lambda = 0\,.$$

For $P < +2$ and $\lambda = 0$ all four roots have non-zero real parts, and this property will persist for λ small (and we are only interested in λ small in this paper). In fact, two eigenvalues have positive real part and two have negative real part. Associated with the eigenvalues with positive (negative) real part is a two-dimensional unstable (stable) subspace. Denote the stable subspace of $\mathbf{A}_\infty(\lambda)$ by

$$\mathrm{E}^s(\lambda) = \mathrm{span}\{\xi_1, \xi_2\}\,.$$

ξ_1, ξ_2 are the eigenvectors associated with the eigenvalues of $\mathbf{A}_\infty(\lambda)$ with negative real part

$$\mathbf{A}_\infty \xi_j = \mu_j \xi_j\,, \quad \mathrm{Re}(\mu_j) < 0\,, \quad j = 1, 2\,, \tag{2.1}$$

with appropriate modification if $\mu_1 = \mu_2$. $\mathrm{E}^u(\lambda)$ is defined analogously. It is easy to verify that $\mathrm{E}^u(\lambda)$ and $\mathrm{E}^s(\lambda)$ are Lagrangian subspaces, and their $x-$dependent extensions are also Lagrangian.

Let $\mathbf{U}^+(x, \lambda)$ be a 4×2 matrix whose columns span the $x-$dependent unstable subspace and so $\mathbf{U}^+(x, \lambda) \to 0$ as $x \to -\infty$. $\mathbf{U}^+(x, \lambda)$ is a path of Lagrangian planes. The Maslov index is defined as the signed count of the intersections of the image of $\mathbf{U}^+$ with E^s as x goes from $-\infty$ to $+\infty$. This definition of the Maslov index for homoclinic orbits is equivalent to the definition introduced in Jones (1988) and Bose & Jones (1995), although here a computable expression for the intersection form is required.

A point x_0 is called a point of one-dimensional intersection between $\mathsf{Image}(\mathbf{U}^+)$ and E^s if

$$\mathsf{Image}(\mathbf{U}^+(x_0, \lambda)) \cap \mathrm{E}^s(\lambda) = \mathrm{span}\{\xi\}\,,$$

for some vector $\xi \in \mathbb{R}^4$. Clearly this implies that

$$\xi = \alpha_1\xi_1 + \alpha_2\xi_2 = \mathbf{U}^+\beta\,,$$

at the intersection for some $\alpha = (\alpha_1, \alpha_2) \in \mathbb{R}^2 \setminus \{0\}$ and $\beta \in \mathbb{R}^2 \setminus \{0\}$. A one-dimensional intersection is regular at x_0 if the crossing is transversal as x is varied. To test for transversality, an intersection form is used.

Formulas for the intersection form have been given in ROBBINS (1991,1992) and ROBBIN & SALAMON (1993). These representations are equivalent (modulo a choice of orientation) and they are based on the following formula. At a point of one-dimensional intersection x_0, the crossing form is defined as:

$$\Gamma(\mathbf{U}^+, \mathrm{E}^s, x_0) = \langle \mathbf{J}\mathbf{U}_x^+\beta, \mathbf{U}^+\beta\rangle \,\mathsf{vol}\,,$$

where vol is the chosen volume form, which is fixed throughout to be

$$\mathsf{vol} = \mathbf{e}_1 \wedge \mathbf{e}_2 \wedge \mathbf{e}_3 \wedge \mathbf{e}_4\,,$$

with $\mathbb{R}^4 = \mathrm{span}\{\mathbf{e}_1, \mathbf{e}_2, \mathbf{e}_3, \mathbf{e}_4\}$.

When $\Gamma(\mathbf{U}^+, \mathrm{E}^s, x_0) \neq 0$, the intersection is said to be *regular*. The *sign of the intersection* is defined as the sign of $\Gamma(\mathbf{U}^+, \mathrm{E}^s, x_0)$.

Using the differential equation and the representation of ξ in (2.1), this is

$$\Gamma(\mathbf{U}^+, \mathrm{E}^s, x_0) = \langle \mathbf{B}(x_0, \lambda)\xi, \xi\rangle \,\mathsf{vol}\,. \tag{2.2}$$

We are now in a position to define the Maslov index of the path $\mathbf{U}^+$. Suppose that

$$\lim_{x\to\pm\infty} \mathsf{Image}(\mathbf{U}^+(x,\lambda)) \cap \mathrm{E}^s(\lambda) = \{0\}\,,$$

and for $-\infty < x < +\infty$ assume that the intersections between $\mathsf{Image}(\mathbf{U}^+)$ and $\mathrm{E}^s(\lambda)$ are one-dimensional (higher-order intersections can also be accounted for but will not be needed here) and regular. Then the Maslov index of the path $\mathbf{U}^+$ is

$$\mathsf{Maslov}(\mathbf{U}^+, \mathrm{E}^s, \lambda) = \sum_{x_0} \mathrm{sign}\,\langle \mathbf{B}(x_0,\lambda)\xi, \xi\rangle\,, \tag{2.3}$$

where the sum is over all points of intersection $-\infty < x_0 < \infty$.

The *Maslov index of the homoclinic orbit* is defined as the limit as $\lambda \to 0^+$,

$$\mathsf{Maslov}^{\mathrm{homoclinic}} = \lim_{\lambda\to 0^+} \mathsf{Maslov}(\mathbf{U}^+, \mathrm{E}^s, \lambda)\,. \tag{2.4}$$

(a) *The role of* λ

The appearance of λ in the formulation appears odd, since we are interested in the Maslov index of homoclinic orbits and this index should be defined purely in terms of the steady equation (1.3). However, the parameter λ is of interest for two reasons. First, it is a stability exponent for the time-dependent equation (1.2). While the issue of stability is only briefly remarked on in this paper, the stability of solitary waves is one of the motivating factors in the study of the Maslov index (cf. JONES (1988), BOSE & JONES (1995), CHARDARD ET AL. (2008)).

The second reason that λ is useful is as a numerical device. When $\lambda = 0$ there is a bounded solution of (1.5) ($\widehat{\mathbf{w}}_x$ in the notation of Appendix A), and so the Maslov index jumps by one at this point. By perturbing λ slightly this property is eliminated. Hence the numerical computations are carried out with λ small. Taking the limit $\lambda \to 0^-$ differs from $\lambda \to 0^+$ but it is merely a convention to decide which limit to take. Here we have opted for the + convention (2.4).

In principle the Maslov index (2.3) is straightforward to compute. We fix λ near 0^+ and integrate the unstable subspace of (1.5) from $x = -L$ to $x = +L$ for some large L and sum the signed intersections. However integration of the unstable subspace is numerically unstable! To avoid this difficulty, the induced equation on $\bigwedge^2(\mathbb{R}^4)$ is integrated and this approach is numerically stable (Allen & Bridges 2002, Chardard et al. 2006, 2008).

3. Exterior algebra representation of Maslov index

The advantage of an exterior algebra representation is that two-dimensional subspaces of $\mathbb{R}^4$ become lines in the exterior algebra space. This strategy reduces the numerical integration to a problem similar to integration on $\mathbb{R}^2$, and then numerical integration is trivial. The details of numerical integration on exterior algebra spaces in this context is given in Chardard et al. (2008) and only the basic details are given here.

$\bigwedge^2(\mathbb{R}^4)$ is a six-dimensional vector space spanned by all non-trivial two-vectors of the form $\mathbf{e}_i \wedge \mathbf{e}_j$, $i, j = 1, \ldots, 4$. The orthonormal basis induced from the standard basis of $\mathbb{R}^4$ is

$$\begin{aligned} \mathbf{E}_1 &= \mathbf{e}_1 \wedge \mathbf{e}_2\,, \quad \mathbf{E}_2 = \mathbf{e}_1 \wedge \mathbf{e}_3\,, \quad \mathbf{E}_3 = \mathbf{e}_1 \wedge \mathbf{e}_4\,, \\ \mathbf{E}_4 &= \mathbf{e}_2 \wedge \mathbf{e}_3\,, \quad \mathbf{E}_5 = \mathbf{e}_2 \wedge \mathbf{e}_4\,, \quad \mathbf{E}_6 = \mathbf{e}_3 \wedge \mathbf{e}_4\,. \end{aligned} \tag{3.1}$$

Any $\mathbf{U} \in \bigwedge^2(\mathbb{R}^4)$ can be represented in the form $\mathbf{U} = \sum_{j=1}^{6} U_j\, \mathbf{E}_j$. An element of $\bigwedge^2(\mathbb{R}^4)$ does not necessarily represent a two-plane. A point $\mathbf{U} \in \bigwedge^2(\mathbb{R}^4)$ represents a two-plane if

$$0 = \mathbf{U} \wedge \mathbf{U} = (U_1U_6 - U_2U_5 + U_3U_4)\,\mathsf{vol}\,.$$

This submanifold of the projectification of $\bigwedge^2(\mathbb{R}^4)$ is the Grassmannian of two-planes in $\mathbb{R}^4$, $\mathrm{G}_2(\mathbb{R}^4)$. A two-plane is Lagrangian if in addition it satisfies

$$0 = \boldsymbol{\omega} \wedge \mathbf{U} = (U_2 + U_5)\,\mathsf{vol}\,,$$

where $\boldsymbol{\omega} = \mathbf{e}_1 \wedge \mathbf{e}_3 + \mathbf{e}_2 \wedge \mathbf{e}_4$ is the two form associated with $\mathbf{J}$.

The practical implementation involves constructing an induced ODE on $\bigwedge^2(\mathbb{R}^4)$. Given the linear system $\mathbf{u}_x = \mathbf{A}(x,\lambda)\mathbf{u}$ on $\mathbb{R}^4$ with $\mathbf{A} = \mathbf{J}^{-1}\mathbf{B}(x,\lambda)$ there is an induced linear system on $\bigwedge^2(\mathbb{R}^4)$,

$$\mathbf{U}_x = \mathbf{A}^{(2)}(x,\lambda)\mathbf{U}\,, \quad \mathbf{U} \in \textstyle\bigwedge^2(\mathbb{R}^4)\,.$$

$\mathbf{A}^{(2)}(x,\lambda)$ is a 6×6 matrix whose entries are linear functions of the entries of $\mathbf{A}(x,\lambda)$. A formula for the entries is given in §2 of Allen & Bridges (2002) and the induced matrix associated with (1.5) is given in Appendix A.

In this setting, the stable subspace at infinity is represented by the two form $\xi_1 \wedge \xi_2$ and the path of unstable subspaces is represented by a two form which will be denoted by $\mathbf{U}^+(x,\lambda)$. It satisfies

$$\mathbf{U}^+_x = \mathbf{A}^{(2)}(x,\lambda)\mathbf{U}^+\,, \quad \text{with} \quad \lim_{x\to-\infty} \mathrm{e}^{-\sigma_+(\lambda)x}\mathbf{U}^+(x,\lambda) = \zeta^+(\lambda)\,, \tag{3.2}$$

where $\zeta^+(\lambda) \in \bigwedge^2(\mathbb{R}^4)$ represents the unstable subspace $\mathrm{E}^u(\lambda)$ and $\sigma_+(\lambda)$ is the sum of the two eigenvalues of $\mathbf{A}_\infty(\lambda)$ with positive real part.

An intersection between $\mathbf{U}^+$ and $\mathrm{E}^s(\lambda)$ can be described as follows. $\mathbf{U}^+$ has a non-trivial intersection with E^s if and only if there exists $\alpha = (\alpha_1, \alpha_2) \in \mathbb{R}^2$ with $\alpha \neq 0$ and

$$\mathbf{U}^+(x,\lambda) \wedge (\alpha_1\xi_1 + \alpha_2\xi_2) = 0\,. \tag{3.3}$$

If $\mathbf{U}^+(x,\lambda) \wedge (\alpha_1\xi_1 + \alpha_2\xi_2) = 0$ implies $\alpha = 0$ then we say that $\mathbf{U}^+(x,\lambda)$ and $\mathrm{E}^s(\lambda)$ are transverse. At a one-dimensional *regular* intersection $\alpha \neq 0$ but it is a one-dimensional subspace of $\mathbb{R}^2$. Intersections can also be checked by monitoring the sign changes of the four-form $\mathbf{U}^+ \wedge \xi_1 \wedge \xi_2$, but the test based on (3.3) is needed for construction of the crossing form.

In the exterior algebra setting a representation of the crossing form is

$$\Gamma(\mathbf{U}^+, \mathrm{E}^s, x_0) = \boldsymbol{\omega} \wedge \xi \wedge \mathbf{A}\xi\,. \tag{3.4}$$

To verify that this is equivalent to (2.2), note that

$$\boldsymbol{\omega} \wedge \mathbf{a} \wedge \mathbf{J}^{-1}\mathbf{c} = \langle \mathbf{a}, \mathbf{c}\rangle\, \mathsf{vol}\,, \quad \text{for any } \mathbf{a}, \mathbf{c} \in \mathbb{R}^4\,.$$

Hence $\boldsymbol{\omega}\wedge\xi\wedge\mathbf{A}\xi = \boldsymbol{\omega}\wedge\xi\wedge\mathbf{J}^{-1}\mathbf{B}\xi = \langle \xi, \mathbf{B}\xi\rangle\,\mathsf{vol}$. The formula (3.4) has an interesting geometric interpretation. At a regular intersection, the two-plane $\xi \wedge \mathbf{A}\xi$ is *not* a Lagrangian plane. It is in the complement to the Lagrangian in $\mathrm{G}_2(\mathbb{R}^4)$.

Suppose that $\lim_{x\to\pm\infty} \mathbf{U}^+(x,\lambda)$ is transverse to $\mathrm{E}^s(\lambda)$, and suppose all the intersections are one-dimensional and regular. Then

$$\mathsf{Maslov}(\mathbf{U}^+, \mathrm{E}^s, \lambda) = \sum_{x_0} \mathrm{sign}\, \boldsymbol{\omega} \wedge \xi \wedge \mathbf{A}\xi\,.$$

The Maslov index of the multi-pulse homoclinic orbit is then obtained by taking the limit $\lambda \to 0^+$.

4. An algorithm for computing the Maslov index

An algorithm for computing the Maslov index based on the exterior algebra representation is constructed as follows. Fix λ. Compute a basis for $\mathrm{E}^s(\lambda)$ and $\mathrm{E}^u(\lambda)$. Earlier, $\mathrm{E}^s(\lambda)$ was expressed as $\mathrm{span}\{\xi_1, \xi_2\}$. Here the stable and unstable subspaces will be represented in the exterior algebra representation. This just means solving

$$\mathbf{A}_\infty(\lambda)\zeta^\pm(\lambda) = \sigma_\pm(\lambda)\zeta^+(\lambda)\,,$$

with $\sigma_+(\lambda)$ ($\sigma_-(\lambda)$) the *sum* of the two eigenvalues of $\mathbf{A}_\infty(\lambda)$ with positive (negative) real part. Then $\zeta^-(\lambda)$ ($\zeta^+(\lambda)$) represents $\mathrm{E}^s(\lambda)$ ($\mathrm{E}^u(\lambda)$).

Integrate (3.2) with the exponential growth $\mathrm{e}^{\sigma_+(\lambda)x}$ factored out†

$$\mathbf{U}^+_x = [\mathbf{A}^{(2)}(x,\lambda) - \sigma_+(\lambda)\mathbf{I}]\mathbf{U}^+\,, \quad -L < x < L\,, \tag{4.1}$$

with

$$\mathbf{U}^+(-L,\lambda) = \zeta^+(\lambda)\,, \tag{4.2}$$

for some large value of L (typically we have used $L = 25$). For the numerical integration a standard fourth-order explicit Runge-Kutta algorithm is used. All the

† Factoring out the exponential growth is purely a numerical device to ensure stable integration.

codes are written in MATLAB. Further details of the numerics including listings of the MATLAB codes can be found in the thesis of CHARDARD (2009).

Intersections are detected and counted as follows. Let

$$Y_j(x,\lambda) = \mathbf{U}^+(x,\lambda)\wedge\xi_j\,,\quad j=1,2\,.$$

Y_1 and Y_2 are three forms and $\bigwedge^3(\mathbb{R}^4)$ is a four dimensional vector space so it is isomorphic to $\mathbb{R}^4$ (this isomorphism can be explicitly constructed but is not needed). An intersection occurs when Y_1 and Y_2 are linearly dependent and, viewed as vectors in $\mathbb{R}^4$, Y_1 and Y_2 are linearly dependent if and only if $Y_1\wedge Y_2=0$. Define

$$y(x,\lambda) = \det\begin{bmatrix}\langle Y_1,Y_1\rangle & \langle Y_1,Y_2\rangle\\ \langle Y_2,Y_1\rangle & \langle Y_2,Y_2\rangle\end{bmatrix}\,. \tag{4.3}$$

Then $Y_1\wedge Y_2=0$ is equivalent to $y(x,\lambda)=0$, or numerically when $y(x,\lambda)<\epsilon$ for some small $\epsilon>0$.

At each intersection, α_1 and α_2 are computed by solving $\alpha_1Y_1+\alpha_2Y_2=0$. α is then used to construct ξ and then the crossing form is evaluated. To summarize: integrate (4.1) with initial condition (4.2) from $x=-L$ to $x=L$. Monitor $y(x,\lambda)$ in (4.3) and when $y(x,\lambda)\approx 0$ compute the sign of the crossing form and add the appropriate sign to the Maslov counter. The Maslov index is then the value of the Maslov counter at $x=L$.

5. Computing the Maslov index for orbits of (1.2)

Apply this theory to the system (1.5) associated with (1.2) linearized about a multi-pulse homoclinic orbit. The induced matrix on $\bigwedge^2(\mathbb{R}^4)$ is given in (A 4) in Appendix A. The system at infinity is hyperbolic for all real λ satisfying $\lambda<1$ (when $P<0$) and $\lambda<1-\frac{1}{4}P^2$ (when $P>0$), and $\mathbf{A}_\infty(\lambda)$ has two eigenvalues with positive real part and two with negative real part. The eigenfunctions associated with $\mathrm{E}^s(\lambda)$ and $\mathrm{E}^u(\lambda)$ are easily calculated.

Before computing branches of multi-pulse homoclinic orbits in the BCT classification, we sketch the properties of the classification. A homoclinic orbit is classified according to the number of times its path in configuration space encircles the origin. The orbit is labelled by $\mathbf{n}(\ell_1,\ldots,\ell_{n-1})$ where n is a natural number called the modality, the number of large local maxima, and ℓ_k is twice the number of encirclings of the origin of configuration space, between consecutive local maxima. A family ψ_P of solutions of (1.3) is said to have a mode at s_P if

$$\lim_{P\to-2^+}(\psi_P(s_{i,P}),\psi'_P(s_{i,P}),\psi''_P(s_{i,P}),\psi'''_P(s_{i,P})) = (\phi_{-2}(0),\phi'_{-2}(0),\phi''_{-2}(0),\phi'''_{-2}(0))\,.$$

A multi-pulse homoclinic orbit is said to have type $\mathbf{n}(\ell_1,\ell_2,\ldots,\ell_n)$ if it has n modes at the points $s_{1,P},s_{2,P},\ldots,s_{n,P}$, and

$$\lim_{P\to-2^+} s_{i+1,P}-s_{i,P}=\infty\,,$$

and the number of zeros of $\frac{1}{2}\psi_P''^2-\frac{1}{2}\psi_P^2+\frac{1}{3}\psi_P^3$ in $[s_{i,P},s_{i+1,P}]$ is equal to $2\ell_i$. BCT have conjectured that there is a unique family of each type, up to a space translation.

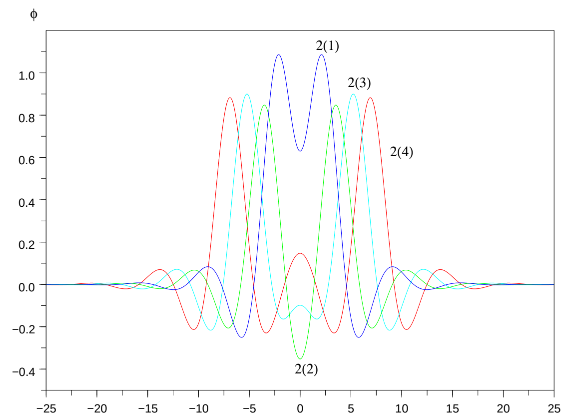

Figure 1. Bimodal multi-pulse homoclinic orbits with $P = 1.5$.

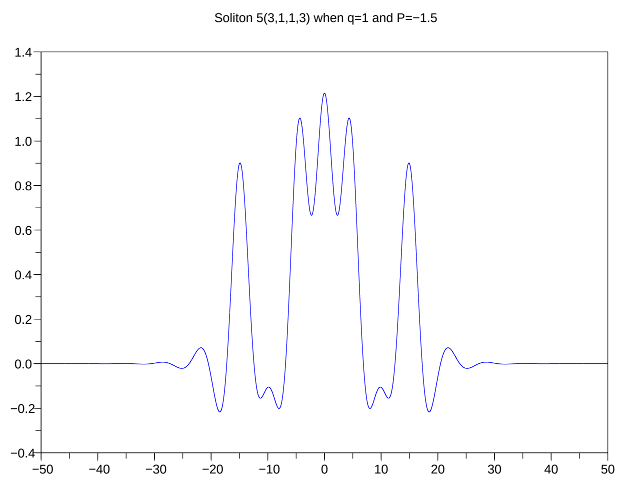

Figure 2. A solitary wave of type $\mathbf{5}(3,1,1,3)$ at $P = 1.5$. The Maslov index is 10.

An important property of this classification is that it is precise only in the limit $P \to -2$. Therefore the strategy for computing a multi-pulse orbit of (1.3) in the BCT classification is to start with an orbit near $P = -2$ and then continue it in P. Examples of bimodal multi-pulse orbits are shown in Figure 1. The $\mathbf{2}(\ell)$ pulses in this figure are all symmetric. They were computed using the shooting algorithm of Champneys & Spence (1993). Indeed, Figure 1 was inspired by Figure 4(a) in Champneys & Spence (1993). An example of a symmetric multi-pulse orbit of modality **5** is shown in Figure 2.

Asymmetric solutions are computed using a Fourier method (approximate the

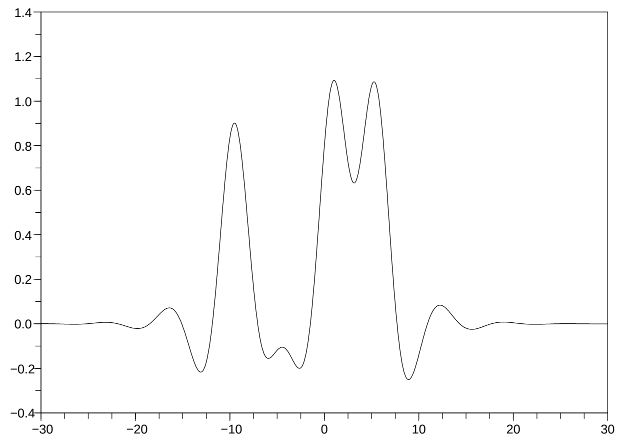

Figure 3. Trimodal solution $\mathbf{3}(3,1)$ when $P = 1.5$. The Maslov index is 6.

homoclinic orbit by a periodic solution of large wavelength). An example of an asymmetric multipulse orbit of type $\mathbf{3}(3,1)$ is shown in Figure 3. The Matlab codes used are listed in the Appendix of Chardard (2009).

We now proceed to compute the Maslov index for a series of multi-pulse orbits. Fixing a multi-pulse orbit in the BCT classification, the Maslov index is computed using the algorithm in §4. To double check the computations, we also computed the Maslov index by approximating the multi-pulse orbit by a periodic solution of long wavelength, and then using the formula in (Chardard et al. 2006, Chardard 2007). See Chardard et al. 2008 for other algorithms for computing the Maslov index. The results for a range of orbits in the BCT classification are listed in Table 1.

The table shows that all computed orbits satisfy the formula (1.1), and so it is reasonable to conjecture that it is true for all multi-pulse orbits in the BCT classification.

There are other examples in the literature of multi-pulse homoclinic orbits that can be identified with the BCT classification and so their Maslov indices can be predicted. The homoclinic orbits found by Champneys & Toland (1993) are of type $\mathbf{2}(\ell)$ and so they have Maslov index 3 (if ℓ is even) or 4 (if ℓ is odd). They were proved to exist for $P \in (-2, -2+\varepsilon)$. Numerical results of Buffoni et al. (1996) suggest that homoclinic orbits of the type $\mathbf{n}(\ell_1, \ldots, \ell_{n-1})$ exists for all $n \geq 2$ and all $P \in (-2, 1.5]$. The homoclinic orbits found by Buffoni (1995) are of type $\mathbf{n}(1, \ldots, 1)$ and hence they have Maslov index $2(n-1)$, and they were shown to exist for all $P \in (-2, 0]$. One can deduce from this that homoclinic orbits of the ODE (1.3) exist with Maslov index of every natural number.

6. Bifurcation and Coalescence

The branches of multi-pulse homoclinic orbits that start at $P = -2$ appear to end at some value of $P < 2$. Buffoni et al. (1996) identified two types of termination

Table 1. *Computed Maslov index for multi-pulse homoclinic orbits in the BCT classification*

Family	Maslov Index
1	2
2(1)	4
2(2)	3
2(3)	4
2(4)	3
2(6)	3
2(7)	4
2(8)	3
2(9)	4
2(10)	3
3(2, 1)	5
3(3, 1)	6
3(1, 1)	6
3(2, 2)	4
3(3, 3)	6

Family	Maslov Index
3(4, 4)	4
3(5, 5)	6
3(6, 6)	4
4(3, 1, 3)	8
4(3, 2, 3)	7
4(3, 3, 3)	8
4(3, 4, 3)	7
4(3, 5, 3)	8
4(3, 6, 3)	7
5(3, 1, 1, 3)	10
5(3, 2, 2, 3)	8
5(3, 3, 3, 3)	10
6(3, 2, 1, 2, 3)	10
6(3, 2, 2, 2, 3)	9
6(3, 2, 3, 2, 3)	10

point: *coalescence* and *bifurcation*. A coalescence corresponds to a turning point and can occur along a symmetric or asymmetric branch. A “bifurcation” in this context is a point where a symmetric branch changes type and has a pitchfork bifurcation to a asymmetric branch. A theory for bifurcation and coalescence using a Lyapunov Schmidt reduction has been developed by Knobloch (1997). In this section we look at the implications of coalescence and bifurcation for the Maslov index. We will concentrate on one example which is illustrative.

The numerics also showed that bifurcation and coalescence often both occur along the same branch. A schematic of Figure 17(c) in Buffoni et al. (1996) is shown in Figure 4. This scenario is an ideal setting to test the implication of the Maslov index. Indeed, we have found a surprising result. Consider the case in Figure 4. We can apply the formula (1.1) to deduce that the branch $\mathbf{4}(2,1,2)$ has Maslov index 6. We confirmed this value numerically. Then after the coalescence point the computations show that the Maslov index jumps to 5. Now, start from the branch $\mathbf{2}(1)$. The formula and numerics show that the Maslov index is 4. Similar use of the formula and computation show that the Maslov indices of the asymmetric $\mathbf{3}(1,2)$ and $\mathbf{3}(2,1)$ branches are also 5. The numerically computed multi-pulse homoclinic orbits emanating from the bifurcation point are shown in Figure 5.

These observations show an interesting anomaly in the BCT classification. The short branch between the coalescence point and the bifurcation point is not classifiable by the BCT scheme. On the other hand, this observation is consistent with the theory of BCT. A branch of multi-pulse homoclinic orbits can only be BCT classified if it can be continued to $P=-2$. It is precisely the branch between the coalescence and bifurcation point that can not be continued to $P=-2$. All other branches in Figure 4 can be continued to $P=-2$. These observations have been obtained numerically. By adapting the theory of Knobloch (1997), Chardard

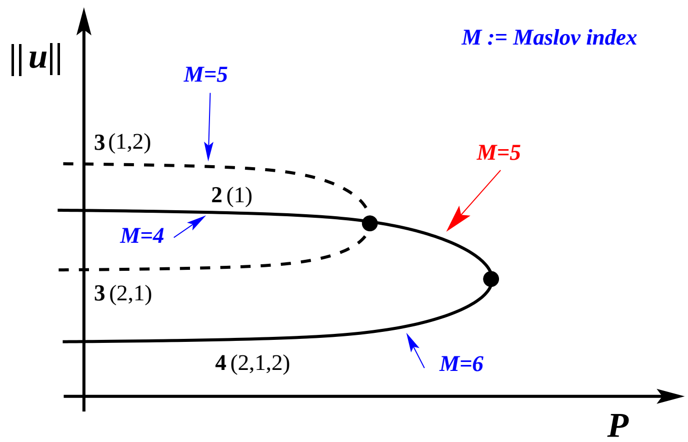

Figure 4. Schematic of Figure 17(c) from Buffoni et al. (1996) with Maslov indices identified.

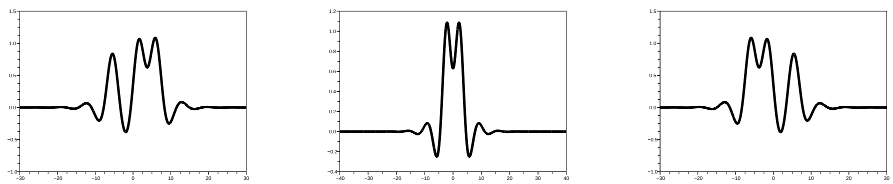

(a) (b) (c)

Figure 5. Orbits $\mathbf{3}(2,1)$, $\mathbf{2}(1)$, $\mathbf{3}(1,2)$ when $P = 1.5$. The branches $\mathbf{3}(2,1)$ and $\mathbf{3}(1,2)$ bifurcate from $\mathbf{2}(1)$ at $P \approx 1.83817$.

(2009) has sketched an argument showing that indeed the Maslov index jumps by one at each bifurcation point and at each coalescence point.

The property of coalescence and bifurcation occuring close together along a branch appears to be pervasive, and so there will be many gaps where the multi-pulse homoclinic orbits are not classifiable by the BCT scheme (see Figure 24 of Buffoni et al.1996). However, all these orbits have a well-defined Maslov index.

7. Remarks on the Morse index and stability of solitary waves

Let

$$\mathscr{L} := \frac{d^4}{dx^4} + P\frac{d^2}{dx^2} + 1 - 2\widehat{\phi}(x)\,.$$

Then (1.4) can be written $\mathscr{L}\phi = \lambda\phi$. Informally, the Morse index of $\mathscr{L}$ is the number of negative eigenvalues of $\mathscr{L}$. To be precise the function space needs to be identified and the spectrum decomposed. Here, just a rough idea of the connection between the Morse and Maslov indices is given. In general the Morse and Maslov indices are not equal. Indeed, one can construct examples where the Morse index is infinite but the Maslov index is finite. On the other hand, the operator $\mathscr{L}$ has a nice structure. It has a monotonicity property which assures that the Maslov index and Morse index are equal (this is proved in Chardard 2009).

With that observation, the role of the Maslov index in stability is quite remarkable. For example, in the Swift-Hohenberg equation (1.2), viewing the multi-pulse homoclinic orbits as stationary localized solitary waves, the Maslov index equals the number of unstable eigenvalues. Therefore one can concude that the higher modality multi-pulse solitary waves – indeed all solitary waves in the BCT classification – are linearly unstable solutions of (1.2), and the higher the modality the more unstable it is.

When this theory is applied to the fifth-order KdV equation however the results are more interesting since high Maslov index solitary waves can still be stable. See Chardard et al. (2008) for results in this direction.

Appendix A. Hamiltonian formulation

The ODE (1.3) can be formulated as a Hamiltonian system in many ways. The Hamiltonian formulation used in the numerics is recorded here. Let

$$q_1 = \phi\,, \quad q_2 = \phi_{xx}\,, \quad p_1 = \phi_{xxx} + P\phi_x\,, \quad p_2 = \phi_x\,,$$

and define

$$H(q,p) = \frac{1}{2}q_1^2 - \frac{1}{2}q_2^2 + p_1p_2 - \frac{1}{2}Pp_2^2 - \frac{1}{3}q_1^3\,.$$

Then (1.3) is represented by the Hamiltonian system

$$\mathbf{J}\mathbf{w}_x = \nabla H(\mathbf{w})\,, \quad \mathbf{w} = (q_1, q_2, p_1, p_2)\,, \tag{A 1}$$

where $\mathbf{J}$ is the standard symplectic operator defined in (1.7).

Let $\widehat{\phi}(x)$ be a solution of (1.3) and $\widehat{\mathbf{w}}$ its associated solution of (A 1),

$$\widehat{\mathbf{w}}(x) := (\widehat{\phi}, \widehat{\phi}_{xx}, \widehat{\phi}_{xxx} + P\widehat{\phi}_x, \widehat{\phi}_x)\,.$$

Then the linearization of (A 1) about $\widehat{\mathbf{w}}$ is

$$\mathbf{J}\mathbf{u}_x = D^2H(\widehat{\mathbf{w}})\mathbf{u}\,,$$

where $D^2H(\widehat{\mathbf{w}})$ is the Hessian of H evaluated at $\widehat{\mathbf{w}}$. Define

$$\mathbf{B}(x,\lambda) = D^2H(\widehat{\mathbf{w}})\mathbf{u} - \lambda\mathbf{I} = \begin{bmatrix} 1 - 2\widehat{q}_1(x) - \lambda & 0 & 0 & 0 \\ 0 & -1 & 0 & 0 \\ 0 & 0 & 0 & 1 \\ 0 & 0 & 1 & -P \end{bmatrix}. \tag{A 2}$$

The linear Hamiltonian system $\mathbf{J}\mathbf{u}_x = \mathbf{B}(x,\lambda)\mathbf{u}$ with $\mathbf{u} \in \mathbb{R}^4$ is the main object of study in the paper. The "system at infinity" is defined by

$$\mathbf{B}_\infty(\lambda) = \lim_{x\to\pm\infty} \mathbf{B}(x,\lambda) = \begin{bmatrix} 1 - \lambda & 0 & 0 & 0 \\ 0 & -1 & 0 & 0 \\ 0 & 0 & 0 & 1 \\ 0 & 0 & 1 & -P \end{bmatrix}. \tag{A 3}$$

Define $\mathbf{A}(x,\lambda) = \mathbf{J}^{-1}\mathbf{B}(x,\lambda)$. Then the matrix induced from $\mathbf{A}(x,\lambda)$ on $\bigwedge^2(\mathbb{R}^4)$ is

$$\mathbf{A}^{(2)}(x,\lambda) = \begin{bmatrix} 0 & 1 & -P & 0 & -1 & 0 \\ 0 & 0 & 0 & 0 & 0 & -1 \\ 1 & 0 & 0 & 0 & 0 & 0 \\ a(x,\lambda) & 0 & 0 & 0 & 0 & +P \\ 0 & 0 & 0 & 0 & 0 & 1 \\ 0 & 0 & -a(x,\lambda) & -1 & 0 & 0 \end{bmatrix}. \tag{A 4}$$

For any $\mathbf{u},\mathbf{v} \in \mathbb{R}^4$ this matrix is defined by

$$\mathbf{A}^{(2)}(\cdot)\mathbf{u}\wedge\mathbf{v} := \mathbf{A}(\cdot)\mathbf{u}\wedge\mathbf{v} + \mathbf{u}\wedge\mathbf{A}(\cdot)\mathbf{u}\,.$$

Details of the construction of induced matrices is given in Allen & Bridges (2002).

References

Allen, L. & Bridges, T.J. 2002 Numerical exterior algebra and the compound matrix method. *Numer. Math.* **92** 197–232.

Arnol'd, V.I. 1967 On a characteristic class entering into conditions of quantization, *Funct. Anal. Appl.* **1** 1–14.

Bose, A. & Jones, C.K.R.T. 1995 Stability of the in-phase travelling wave solution in a pair of coupled nerve fibers. *Indiana Math. J.* **44**, 189–220.

Buffoni, B. 1995 Infinitely many large amplitude homoclinic orbits for a class of autonomous Hamiltonian systems, *J. Diff. Eqns.* **121** 109–120.

Buffoni, B., Champneys, A.R. & Toland, J.F. 1996 Bifurcation and coalescence of a plethora of multi-modal homoclinic orbits in a Hamiltonian system. *J. Dyn. Diff. Eqns.* **8** 221–281.

Burke, J. & Knobloch, E. 2007 Homoclinic snaking: structure and stability. *Chaos* **17** 037102.

Champneys, A.R. 1999 Homoclinic orbits in reversible systems and their applications in mechanics, fluids and optics, *Physica D* **112**, 158–186.

Champneys, A.R. & Spence, A. 1993 Hunting for homoclinic orbits in reversible systems: a shooting technique, *Adv. Comp. Math.* **1** 81–108.

Champneys, A.R. & Toland, J.F. 1993 Bifurcation of a plethora of multi-modal homoclinic orbits for autonomous Hamiltonian systems *Nonlinearity* **6** 665–721.

Chardard, F. 2007 Maslov index for solitary waves obtained as a limit of the Maslov index for periodic waves. *C. R. Acad. Sci. Paris, Ser. I* **345** 689–694.

Chardard, F. 2009 Stabilité des Ondes Solitaires, *PhD Thesis*, École Normale Supérieure de Cachan, France.

Chardard, F., Dias, F. & Bridges, T.J. 2006 Fast computation of the Maslov index for hyperbolic linear systems with periodic coefficients. *J. Phys. A: Math. Gen.* **39**, 14545–14557.

Chardard, F., Dias, F. & Bridges, T.J. 2008 Computing the Maslov index of solitary waves. Part 1: Hamiltonian systems on a four-dimensional phase space. *Preprint*†.

Chen, C.-N. & Hu, X. 2007 Maslov index for homoclinic orbits of Hamiltonian systems. *Ann. Inst. H. Poincaré Anal. Non Linéaire* **24** 589–603.

† Electronic preprint available at `http://www.cmla.ens-cachan.fr/Membres/chardard.html`

Jones, C.K.R.T. 1988 Instability of standing waves for non-linear Schrödinger-type equations. *Ergodic Theory Dyn. Sys.* **8***, 119–138.

Knobloch, J. 1997 Bifurcation of degenerate homoclinic orbits in reversible and conservative systems, J. Dyn. Diff. Eqns. **9** 427–444.

Littlejohn, R.J. 1986 The semiclassical evolution of wave packets. *Phys. Rep* **138**, 193–291.

Littlejohn, R.G. & Robbins, J.M. 1987 New way to compute Maslov indices. *Phys. Rev. A* **36** 2953–2961.

Peletier, L.A. & Troy, W.C. 2001 *Spatial Patterns: Higher-Order Models in Physics and Mechanics*, Springer: Berlin.

Pletyukhov, M. & Brack, M. 2003 On the canonically invariant calculation of Maslov indices. *J. Phys. A* **36** 9449–9469.

Robbin, J.W. & Salamon, D.A. 1993 The Maslov index for paths. *Topology* **32**, 827–844.

Robbins, J.M. 1991 Maslov indices in the Gutzwiller trace formula, *Nonlinearity* **4**, 343–363.

Robbins, J.M. 1992 Winding number formula for Maslov indices. *Chaos* **2**, 145–147.